

PORTABLE BIOMEDICAL MEASUREMENT DEVICES:  
MOBOSENS AND IMPEDANCE SENSING SYSTEMS

BY

HAN ZHANG

THESIS

Submitted in partial fulfillment of the requirements  
for the degree of Master of Science in Electrical and Computer Engineering  
in the Graduate College of the  
University of Illinois at Urbana-Champaign, 2016

Urbana, Illinois

Adviser:

Associate Professor Gang Logan Liu

## **ABSTRACT**

Human health has become a very important topic as society pays more attention to the people's quality of life. Therefore, wearable devices with the capability of monitoring various human health indexes and detecting environmental pollution metrics are in great demand.

In this thesis, two methods will be discussed in detail. One method that has been developed to perform the tests is called electrochemical sensing, 'MoboSens'. It uses a smartphone as its sensing platform with an integrated plug-and-play microelectronic ionic sensor, and the whole package is connected through the audio jack on the smartphone. It is used to measure nitrate concentration in water portably. The other method is called impedance sensing measurement. A portable device is used as the platform to combine with the impedance-based sensing technologies. It is designed to detect some species of *Escherichia coli* and *Salmonella* bacteria. The work discusses the system-level circuit design for the prototypes of both methods. The testing results from these two sensing methods have been confirmed with other existing analytical testing methods.

## ACKNOWLEDGMENTS

First of all, I would like to express my highest gratitude to my master's adviser, Professor Gang Logan Liu, for his invaluable guidance, patience and advice. He offered me the opportunity and the platform to pursue my master's degree and conduct research in system design at the University of Illinois at Urbana-Champaign.

Second, I would like to thank all the group members in Liu's Nanobionics Laboratory, particularly Jing Jiang, Xinhao Wang, Xiangfei Zhou and Yukun Ren, for their help, suggestions and discussions about projects. Also, thanks to Bobi Shi, an undergraduate student who helped me with impedance measurement and testing. I would like to thank the staff members working in the ECE Electronics Services shop for their patience and technical guidance.

Finally, I would like to express my sincere appreciation to my family and friends, especially my girlfriend Shenjia Shi, for all the love, patience and support along the way.

# TABLE OF CONTENTS

|           |                                                                    |    |
|-----------|--------------------------------------------------------------------|----|
| CHAPTER 1 | INTRODUCTION .....                                                 | 1  |
| 1.1       | <i>Electrochemical Sensing Background</i> .....                    | 1  |
| 1.2       | <i>Two-Electrode System vs. Three-Electrode System</i> .....       | 2  |
| 1.3       | <i>Impedance Sensing Background</i> .....                          | 4  |
| 1.4       | <i>Technical Background for Impedance Measurement</i> .....        | 5  |
| CHAPTER 2 | MOBOSENS SYSTEM-LEVEL INTEGRATION.....                             | 7  |
| 2.1       | <i>Overview</i> .....                                              | 7  |
| 2.2       | <i>Demodulation Unit</i> .....                                     | 10 |
| 2.3       | <i>Potentiostat Unit</i> .....                                     | 14 |
| 2.4       | <i>Modulation Unit</i> .....                                       | 16 |
| 2.5       | <i>Power Management Unit</i> .....                                 | 17 |
| 2.6       | <i>Multi-Sensing Sub-Unit</i> .....                                | 20 |
| CHAPTER 3 | IMPEDANCE SENSING SYSTEM-LEVEL INTEGRATION .....                   | 22 |
| 3.1       | <i>Overview</i> .....                                              | 22 |
| 3.2       | <i>AD5933 – 12-Bit Impedance Converter, Network Analyzer</i> ..... | 24 |

|                                         |                                                   |    |
|-----------------------------------------|---------------------------------------------------|----|
| 3.3                                     | <i>Other Units and Components in System</i> ..... | 26 |
| 3.4                                     | <i>Result</i> .....                               | 28 |
| CHAPTER 4 SUMMARY AND FUTURE WORK ..... |                                                   | 33 |
| REFERENCES.....                         |                                                   | 34 |

# CHAPTER 1

## INTRODUCTION

### 1.1 Electrochemical Sensing Background

Nitrogen is an essential chemical element on Earth. It plays an important role in forming some organic particles, such as nucleic acids and amino acids [1]. However, excessive nitrogen could have adverse effects on human health and the environment, especially nitrite ( $\text{NO}_2^-$ ), which is known to poison fish and to be harmful to human health [2]. Thus, it is necessary to have an effective solution for nitrate concentration detection. Since detecting invisible contaminants in water requires special equipment and chemicals, people are not able to perform the test in normal daily life. A smartphone platform with easy operation could be a breakthrough for nitrate detection because people could then detect contaminants in water with only a smartphone.

Comparing with some existing methods for nitrate concentration determination, such as spectroscopic and chromatography, the electrochemistry method is comparatively easy to apply on a portable device [3]. Oxidation reaction or reduction reaction happens based on the voltage potential between reference and working electrodes in the electrochemical method.

MoboSens is a mobile sensing system used for electrochemical sensing of nitrate concentration measurement. It includes an electrochemical sensor, a control circuit and a mobile application.

The control circuit board has a small form factor, so that the whole system can be portably used. In contrast to other smartphone-based sensing platforms, MoboSens applies the audio jack as its sensing interface instead of using a camera. Under this situation, the smartphone can not only retrieve but also send signals. The other reason for using audio jack for transmitting input and output signals instead of using the USB port is that all mobile phones do not have uniform USB port design [4, 5]. This thesis presents the system and circuit design for the whole MoboSens package, and the system-level implementation will be mainly discussed in Chapter 2.

## **1.2 Two-Electrode System vs. Three-Electrode System**

Traditionally, an electrochemical sensing system uses two electrodes: a working and a reference electrode. In the two-electrode system, electrochemical reaction appears at the working electrode. Due to the electron transfer in the reaction, the material of the working electrode should be sensitive to the oxidation-reduction target. The role of the reference electrode is to provide a constant potential and to pass the current during reactions. However, the limitation of the two-electrode system is very obvious. The current flowing through the reference electrode leads to depolarization over time, which leads to a voltage drift around the reference electrode so that the potential is no longer stable. This small drift may result an inaccurate measurement.

Today, there is an electronic instrument called a potentiostat, which is used for electrochemical cell measurement [6]. The potentiostat uses the three-electrode system. Similar to the two-electrode system, the three-electrode system also has a working and a reference electrode. The

third electrode is called an auxiliary or counter electrode. The counter electrode would inject current into the electrochemical cell. Thus, the three-electrode system controls both the current through the counter electrode and the voltage difference between the working electrode and the reference electrode. It measures the current flowing between the working electrode and the counter electrode [6]. Thus, it helps to ensure the stable potential of the reference electrode without any current flowing through it. A simple schematic of a potentiostat is shown in Figure 1.1, which indicates how those electrodes perform their functionalities.

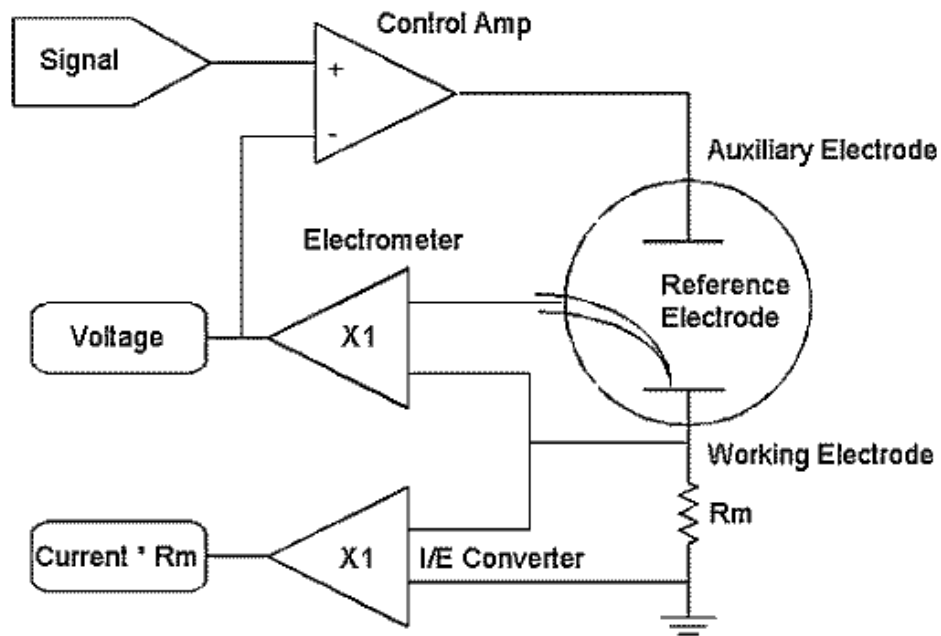


*Figure 1.1: Simple schematic of a potentiostat [6]*



### 1.3 Impedance Sensing Background

As the quality of life improves in many developed and developing countries, people become more concerned whether their food or water has been contaminated with harmful bacteria. Some species of *E. coli* and other bacteria in food and water can cause very severe health conditions. In contrast to electrochemical sensing which is used to measure for electrochemical cells, impedance sensing can be used for detecting bacteria for biomedical diagnostics.

In Wikipedia, it is said that “Electrical impedance is the measure of the opposition that a circuit presents to a current when a voltage is applied” [7]. Since impedance of a material is a result of its reaction to an applied voltage, it can be utilized to characterize material properties. Schwan has a great contribution for modern bioengineering [8], particularly on electrical properties of cells and tissue. Schwan’s research was the first time to demonstrate that the alternating current (AC) electrical measurement can be applied for biomedical diagnostics [9]. To detect the impedance characteristics of the target material, AC voltage is applied under a range of variable frequencies.

The portable impedance sensing device applies the embedded impedance sensing technology integrated circuit (IC) chip and an Arduino as the microcontroller board. Bluetooth is used for data communication to talk to computers or other devices. The whole device is powered by a rechargeable Li-ion battery, which can be recharged through a USB port. Due to its small form factor, the whole system can be portably used for biomedical detection. This thesis will focus on the system and circuit design for the whole impedance sensing package, and the system-level implementation will be mainly discussed in Chapter 3.

## 1.4 Technical Background for Impedance Measurement

According to [10], “impedance ( $Z$ ) is generally defined as the total opposition a device or circuit offers to the flow of an alternating current AC at a given frequency. Its value is equal to the ratio between the voltage and the current over an element of a circuit. Therefore, the unit of impedance is ohm ( $\Omega$ ). Impedance is represented as a complex quantity which is graphically shown on a vector plane.”

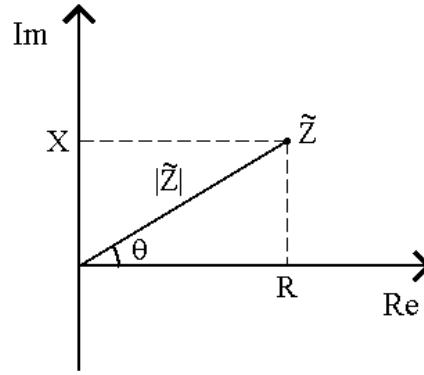


Figure 1.2: A graphical representation of the complex impedance plane [11]

As Figure 1.2 shows, an impedance can be represented in rectangular coordinate form  $R + jX$ , where  $R$  is the resistance as the real part and  $X$  is the reactance as the imaginary part. From this impedance plane, we can derive the relation equations for  $R$ ,  $X$ ,  $Z$  and  $\theta$ :

$$R = |Z| \cos\theta \quad (1.1)$$

$$X = |Z| \sin\theta \quad (1.2)$$

$$|Z| = \sqrt{R^2 + X^2} \quad (1.3)$$

$$\theta = \tan^{-1}\left(\frac{X}{R}\right) \quad (1.4)$$

The polar coordinate expression  $|Z|\angle\theta$  is usually calculated as the impedance measurement because it directly provides the information of its amplitude attenuation and phase shift.

## CHAPTER 2

### MOBOSENS SYSTEM-LEVEL INTEGRATION

#### 2.1 Overview

The overall block diagram is shown in Figure 2.1. From the block diagram, we can see that the signal input and output are transmitted through the audio jack on the smartphone due to the uniformity in design and availability for all smartphones. The external circuit board and sensor strip have small form factors, which allow the customers to use it portably.

The whole nitrate detection process sequence is also shown in Figure 2.1. First of all, since the smartphone can hardly produce a voltage sweep as the output, it generates a frequency sweep through its speaker with the embedded digital-to-analog module. To drive the nitrate electrochemical sensor, we need a frequency demodulation component to convert the frequency sweep to a voltage sweep. Then, after flowing through the sensor strip, the output voltage signal should be converted to a frequency output by using a frequency modulation component. The reason for this process is that the microphone can only receive a signal within a certain voltage limitation but a large frequency limitation. Without the frequency modulation component, most of the signal will get truncated which causes loss of information. Also, the modulation and demodulation help to match the frequencies between the smartphone and the nitrate sensor strip.

Next, the frequency output is retrieved by the microphone with the embedded analog-to-digital module.

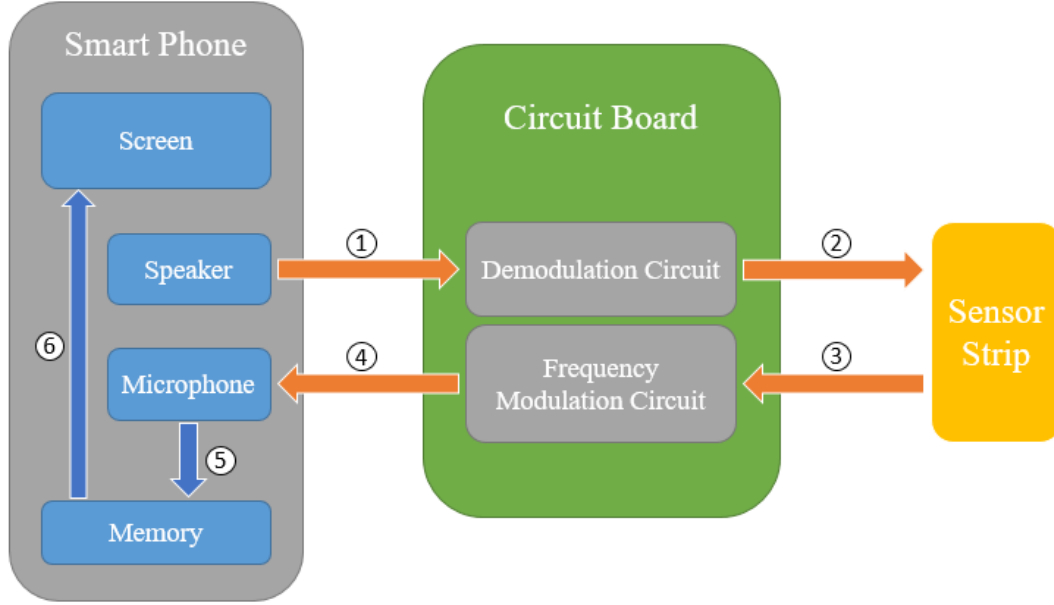


*Figure 2.1: Block diagram and operation sequence of MoboSens system. (1) Signal with a frequency sweep is generated from the speaker on the smartphone to the demodulation unit on the external circuit board. (2) A voltage sweep is generated from the demodulation unit, and passed for cyclic voltammetry testing. (3) The output current signal from sensor strip is converted to a voltage signal, and the voltage signal is sent to the frequency modulation unit. (4) The signal gets modulated to a frequency output signal and sent to the microphone on the smartphone. (5) The raw frequency output data is retrieved and stored in the memory. (6) A plot for frequency in time domain is displayed on the smartphone screen.*

After the signal is passed into the smartphone, a smartphone-based software application is developed to drive the raw data. In the application, we can choose to perform a real-time calibration or use the stored calibration curve to compute the information for nitrate

9

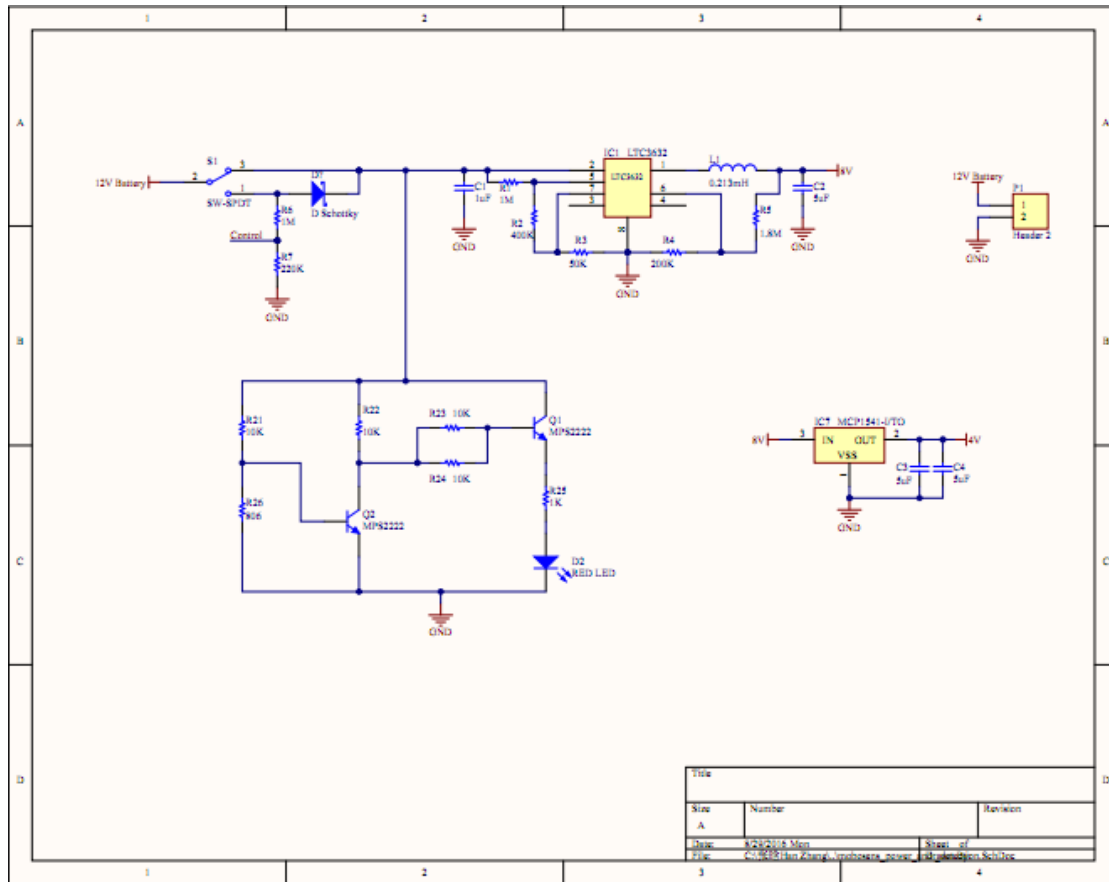
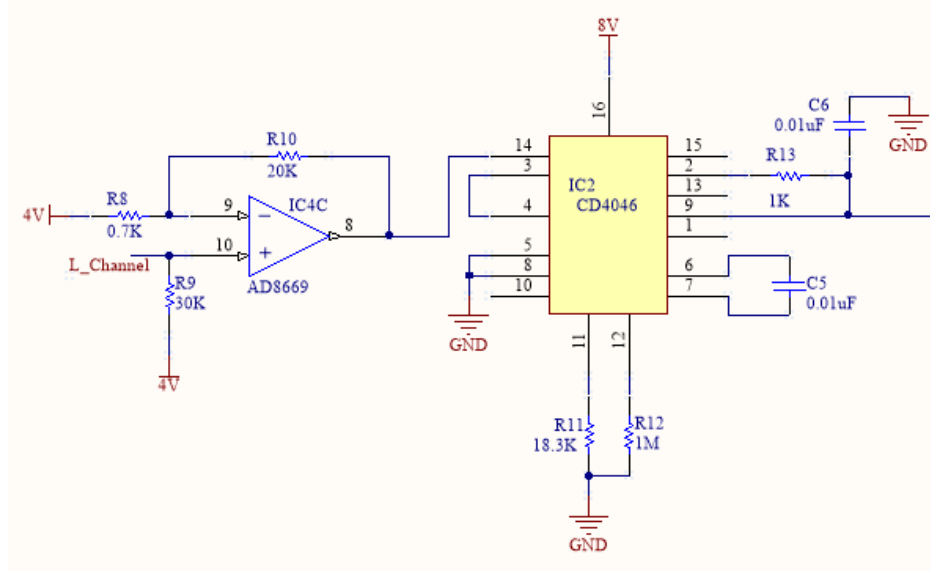


Figure 2.3: Power control circuit schematic for MoboSens system

## 2.2 Demodulation Unit

The circuit schematic for the demodulation unit is shown in Figure 2.4. From the schematic, the input signal is connected with the left channel of the audio jack on the smartphone, which is the speaker. There are some limitations for the speaker characterization: the maximum peak-

to-peak voltage of the generated sine wave from the speaker is about 1 V, and the frequency range is from 20 Hz to 20 kHz.



*Figure 2.4: Demodulation unit schematic*

To perform the frequency demodulation, an IC chip from TI is used (CD4046). This chip is a CMOS micro-power phase-locked loop (PLL) consisting of a low-power, linear voltage-controlled oscillator (VCO) and two different phase comparators [12]. Figure 2.5 shows the block diagram for the chip CD4046. By using this IC chip, its PLL and VCO could help to convert the input signal with a frequency sweep to a voltage sweep output signal.



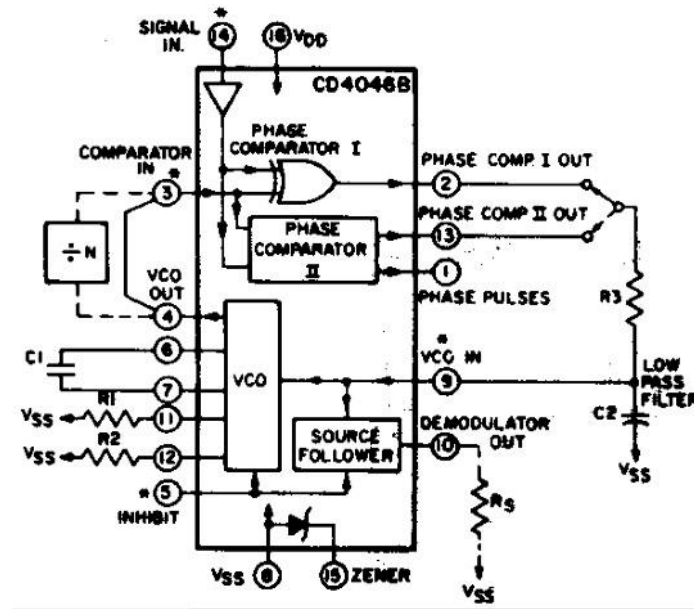


Figure 2.5: CD4046 CMOS phase-locked loop block diagram [12]

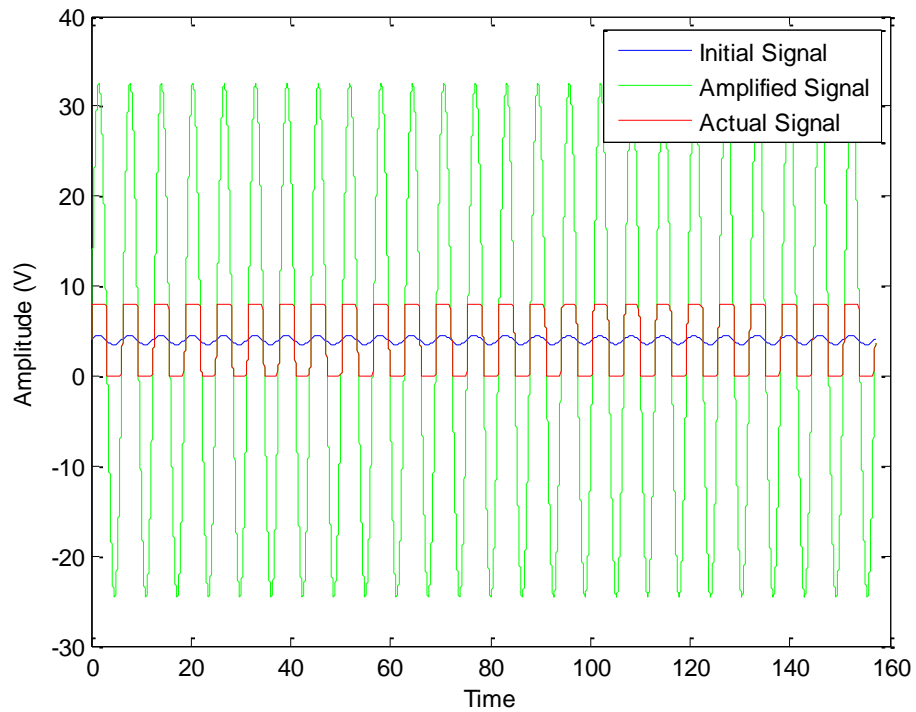


Figure 2.6: Matlab simulation for voltage signal from speaker.

However, according to the datasheet, it is good to have a square wave signal as the input. Thus, it turns out that an operational amplifier (op-amp) is used to generate a square wave from a sine wave. To perform this transit, the sine wave signal needs to be amplified many times. Then, due to the supply voltage limitation, most of the signal will get truncated, so the remaining signal passing to the demodulation unit seems like a “square-like” wave. The simulation plot generated by Matlab is shown in Figure 2.6, which straightforwardly shows what the output looks like. The blue signal is the initial sine wave with 1 V peak-to-peak amplitude from the speaker. The green signal is the amplified signal, which is 30 times the initial signal. The red signal is the actual signal that comes from the op-amp, which is truncated by the op-amp supply voltage.

The op-amp used in the system is an IC chip with the part number AD8669 from ADI. This IC chip has very good performance with low noise and precision, which are very important for electrochemical measurements [13]. Also, the other main reason to use it is that this IC chip is a rail-to-rail op-amp with large CMRR value. Normally, the input common-mode voltage range and output voltage swing are 2 V less than the total supply voltage range. With a rail-to-rail op-amp, the input and output voltages can be operated to swing very close to the supply rails, so that the signal voltage capability is maximized to the limited supply voltage. For MoboSens, the level of the supply voltage for op-amps can be lowered to increase its lifetime by using battery power.

Even though the op-amp can be powered by dual supplies, a single supply power is used for MoboSens due to its simplicity. Otherwise, another inverting regulator will be needed for generating the negative supply voltage. Because it is a single-supply op-amp, the reference

ground voltage is raised to 4 V. It will be discussed in section 2.3 for this reason. Thus, the ground voltage for the audio jack is raised to 4 V as well.

### 2.3 Potentiostat Unit

After the signal gets demodulated, it is passed to the sensor strip for electrochemical reactions. Because it uses a three-electrode system, which has the same functionality as a potentiostat, this part is called the potentiostat unit. The circuit schematic for this unit is shown in Figure 2.7.

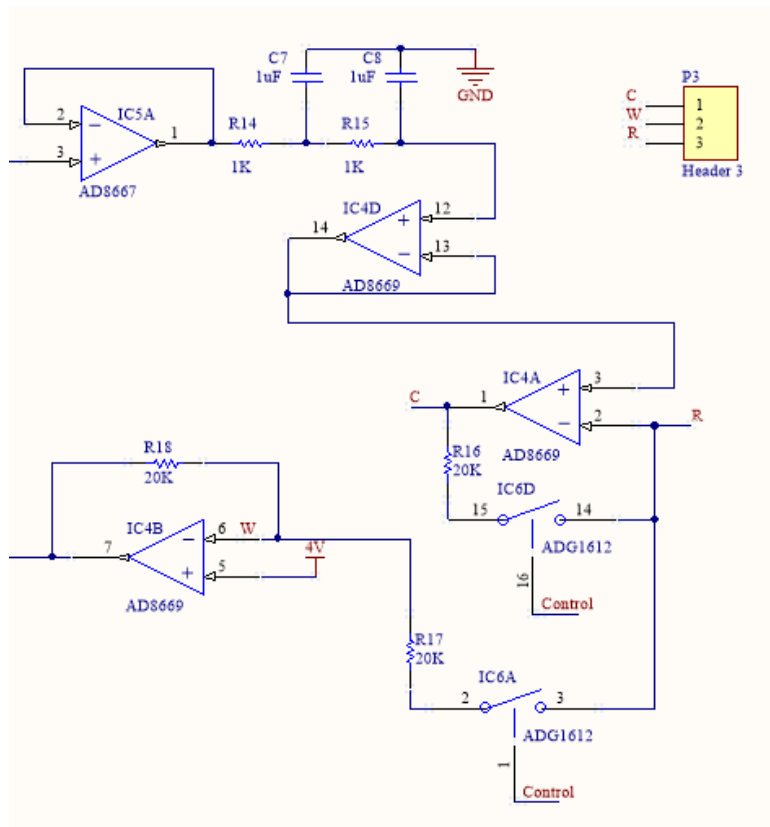


Figure 2.7: Potentiostat unit schematic

The input of this unit is directly connected with the output of the demodulation unit. Although the CD4046 has an internal voltage follower, it is safe to introduce another external voltage buffer to isolate the circuits for preventing circuitry interference. Then, a two-stage low-pass filter is applied to filter out the noise generated from the CD4046 and to get a relatively pure DC voltage. Another voltage buffer is implemented right before the potentiostat circuit for isolation.

From the schematic shown in Figure 2.7, the sensor strip will be connected to the system through the Header 3 by inserting to the corresponding electrodes. When a voltage sweep is applied from the CD4046, the cyclic sweeping voltage is then added to the reference potential, which is labeled as R in the figure. Since the working electrode is connected to the reference ground, which is 4 V, the voltage potential between the working electrode and reference electrode is generated. Also, due to the very high impedance looking into the input of the op-amp, it will not allow any current to flow through the reference electrode. Oppositely, since the counter electrode is connected to the output of the op-amp, it can generate current as much as needed, like a current source. Now, the circuitry works as a potentiostat with three electrodes. By inserting a resistor between the working electrode and the output for that op-amp, the current flowing through the electrochemical cell can be converted to voltage information.

Since the CD4046 chip needs to be calibrated for nitrate samples with different concentrations, a calibration strip is required to perform the process. Two 20 k $\Omega$  resistors are utilized as the calibration strip. To make this calibration strip embedded with the system, an analog switch, whose part number is ADG1612 from ADI, is added to the potentiostat unit. Thus, when the switch is on, the system goes to calibration mode; when the switch is off, all of the three

electrodes are not connected until the sensor strip is presented. To control this analog switch, more detail will be discussed in section 2.5.

During the nitrate measurement, a sine wave with frequency increasing from 5300 Hz to 7600 Hz and decreasing from 7600 Hz to 5300 Hz is generated from the smartphone audio jack. 5300 Hz and 7600 Hz respectively correspond to 0 V and -1.8 V for the voltage difference between working and reference electrodes. When the signal has 7600 Hz frequency, the reference electrode should be 1.8 V compared with the working electrode voltage. At this point, the voltage at the counter electrode should be 3.6 V compared with the working electrode voltage since the current flows from the counter electrode. In this process, the oxidation reaction is prior to the reduction reaction. However, for other electrochemical cell measurements, the reduction reaction may happen prior to the oxidation reaction, which means the sine wave signal frequency might be lower than 5300 Hz. For both considerations, 4 V is selected as the reference ground voltage. Thus, it is better to have 8 V for the supply voltage of the op-amps.

## **2.4 Modulation Unit**

The peak-to-peak voltage of the output signal should be within 200 mV, and the frequency limit for this signal is between 20 Hz and 10 kHz. Obviously, it is impossible to connect the potentiostat unit directly to the microphone because the signal from the potentiostat is a DC voltage sweep with a frequency of 0.033 Hz. Due to the signal limitation for the microphone on the smartphone, a modulation unit is desired in the system. The schematic for the modulation unit is shown in Figure 2.8.

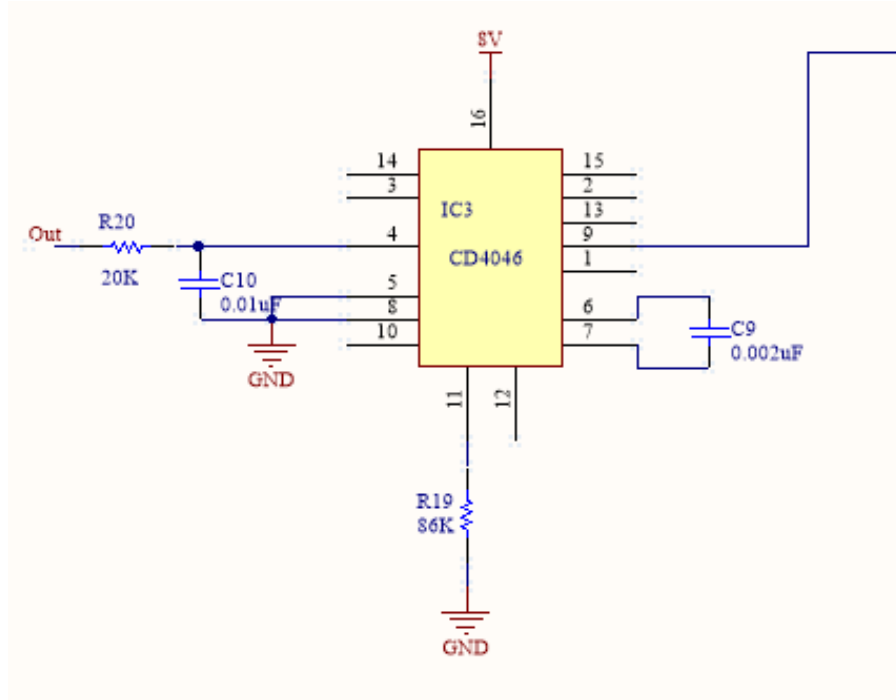


*Figure 2.8: Modulation unit schematic*

The CD4046 is used again for the frequency modulation by using its internal VCO [12]. A 20 k $\Omega$  resistor is inserted between the microphone and the output from the CD4046, because the output signal from the CD4046 has larger peak-to-peak amplitude than 200 mV. To avoid the information loss, we have to shrink the amplitude of the signal within 200 mV.

## 2.5 Power Management Unit

All the components and system need to be powered while in use. For the MoboSens system, two 12 V batteries in parallel are used for supplying the power. As the previous sections mentioned, all the op-amps and IC chips need 8 V for their DC supply voltage. Also, a standard

4 V is required as the reference ground for the audio jack. Moreover, there is a battery voltage monitor to detect if the voltage is below the threshold, so that the dead batteries can be replaced for the normal system operations. Figure 2.9 shows the schematic for the power management unit.

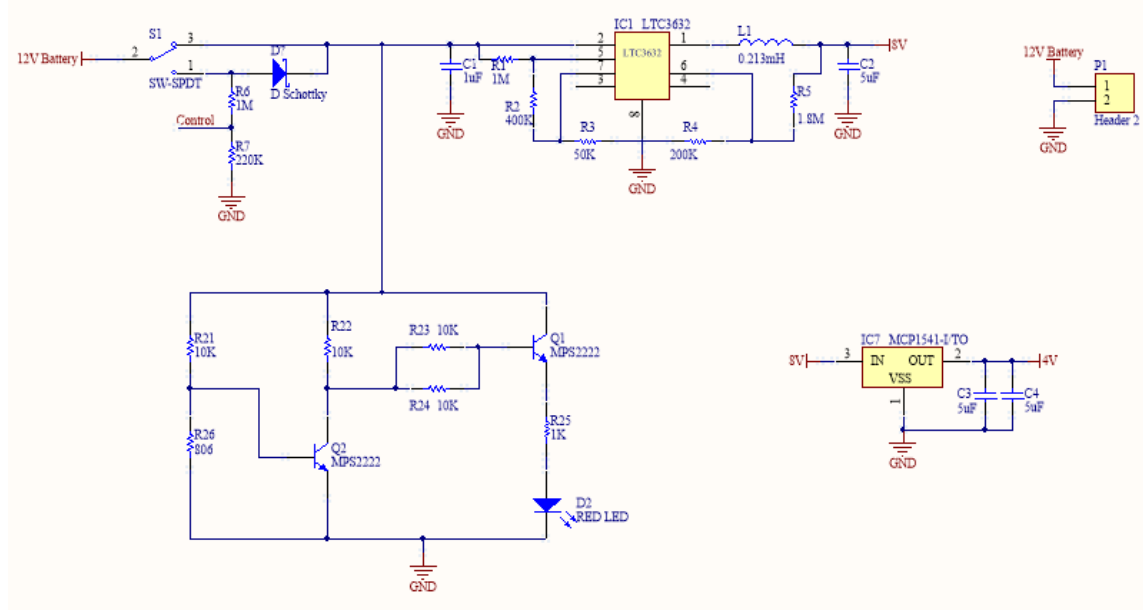


Figure 2.9: Power management unit schematic

A linear regulator was chosen to deliver a standard 4 V due to its simplicity. The input for the linear regulator is a constant 8 V voltage. For generating a standard 8V, an IC chip from LTC with a part number of LTC3632 is used. This chip is a buck converter, which is a step-down switching regulator. Since the electrochemical measurement may take a several cycles to process, including the calibration and settling cycles, a longer battery life for the system is very important. Although linear regulators are easy to implement at low prices, switching regulators can achieve a much higher power efficiency to save power and extend the system lifetime. With

a 3 k $\Omega$  load resistor, the power efficiency for the LTC3632 was verified, and the measurement data is tabulated in Table 2.1. (Note: Since the resistor combination with desired values could not be found in the Services Shop in school for generating the 8 V output, an 8.4 V was produced as the regulator output.)

Table 2.1: Power Efficiency for Converting 12V to 8.4V by Using the LTC3632

| $V_{in}$ (V) | $V_{out}$ (V) | $I_{in}$ (mA) | Efficiency (%) |
|--------------|---------------|---------------|----------------|
| 12.11        | 8.398         | 2.22          | 87.4447        |
| 12.00        | 8.408         | 2.24          | 87.6667        |
| 10.73        | 8.409         | 2.43          | 90.3985        |
| 9.75         | 8.42          | 2.63          | 92.16          |
| 9.02         | 8.41          | 2.787         | 93.7837        |
| 8.47         | 8.416         | 2.91          | 95.7886        |

There is a three-way slide switch in the system, whose function is on-off-on. Because the calibration resistors are embedded in the system, the three-way switch enables the users to control three states: calibration only, system power off, and sensor strip testing. When the switch is on the calibration mode, the battery is connected with a voltage divider to generate a DC control signal with at least 2 V for the analog switch shown in section 2.3. Then, the voltage passes a Schottky diode, which has a small turn-on voltage for energy saving. When the slide switch is on the sensor strip mode, the battery is directly connected with the buck converter. The Schottky diode will block the signal to the voltage divider, so that the control signal to the analog switch will stay low. Last, when the slide switch is on power-off mode, the battery is disconnected with all the components, and the whole system is off.



The battery voltage monitor applies two NPN bipolar junction transistors (BJTs) and a red LED as the indicator. When the battery voltage is below around 8.5 V, the LED is on, which tells one to replace the batteries. The circuitry is very simple. When the battery voltage is larger than the threshold, the left BJT is on, and it will pull down the base voltage of the right BJT. Thus, the right BJT is off, and no current can flow through the LED, which means the LED is off. When the battery voltage is lower than the threshold, the base voltage for the left BJT is not enough to turn it on. Thus, the right BJT turns on due to the high base voltage, and it turns on the LED.

## **2.6 Multi-Sensing Sub-Unit**

Since the MoboSens system only uses the left channel of the audio jack on the smartphone, the other channel can be implemented as well. For the MoboSens system, only one sensor strip can be measured each time. Every time, when a new electrochemical cell is ready to be measured, it requires the users to unplug the old sensor strip and plug in the new one. To simplify the procedure, the right channel can be used for generating the selecting bits for an analog multiplexer to choose. Thus, the user can insert all the testing sensor strips into the external device, and the analog multiplexer decides which sensor strip can connect to the system. Figure 2.10 shows the circuit schematic to achieve the selecting performance.

First of all, since the right channel of the speaker generates an AC signal, a RC high-pass filter is connected with the right channel. With this HPF, the output for a signal with its frequency smaller than the cutoff frequency will be zero; the output for a signal with its frequency higher

than the cutoff frequency can remain its signal. Then, the output signal flows through a rectifier so that the output should be a DC voltage. By applying two inverting Schmitt triggers after, the output is pure digital, and it is the clock for the first J-K flip-flop. Next, the second J-K flip-flop uses the inverting output from the first J-K flip-flop as its clock. From the datasheet [14], we can see when ‘JK’ is ‘10’, it is toggle action, which means the output will change when the rising edge occurs for both J-K flip-flops. Thus, by altering the frequency of the original signal from the right channel, we can set the clock for the first J-K flip-flop, which also controls the second J-K flip-flop. The output pins labeled in the figure Q1 and Q0 are the selecting bits for a 1-to-4 analog multiplexer.

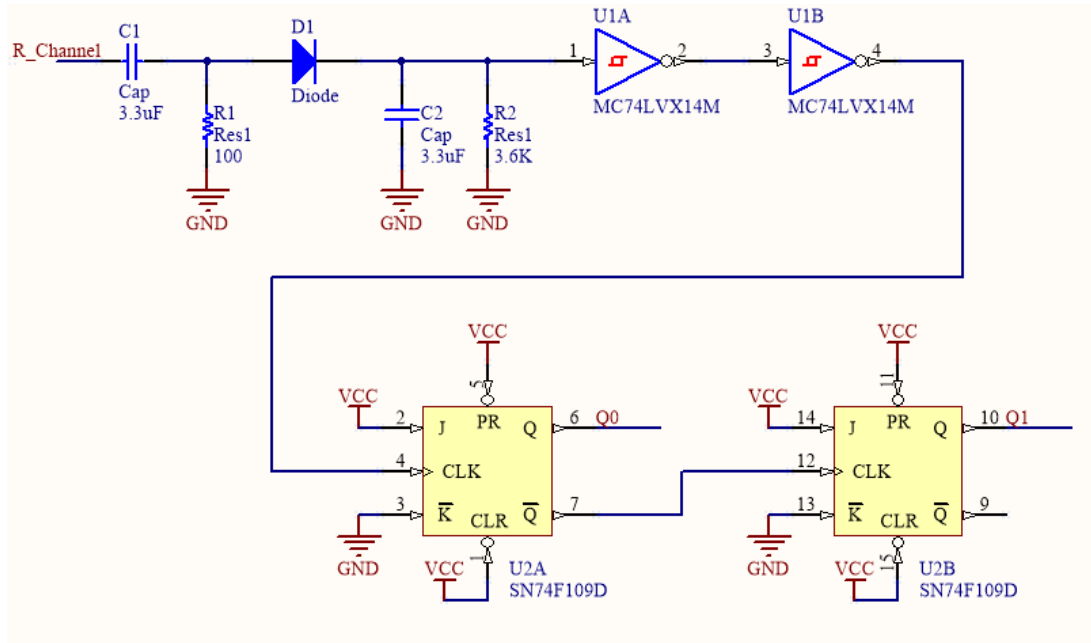


Figure 2.10: Multi-sensing sub-unit schematic

## CHAPTER 3

### IMPEDANCE SENSING SYSTEM-LEVEL INTEGRATION

#### 3.1 Overview

The overall block diagram is shown in Figure 3.1. An Arduino UNO board acts as the control board. All the control signals can be sent to the circuit board through GPIO pins. The I2C port is used to collect the impedance result from the impedance analyzer. Since it can be used portably, all the measurement information can be wirelessly communicated to other devices, like computers, through Bluetooth.

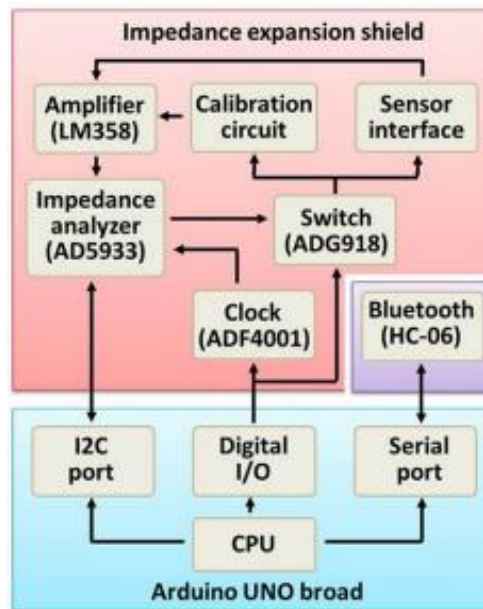


Figure 3.1: Block diagram of impedance sensing system [15]



### 3.2 AD5933 – 12-Bit Impedance Converter, Network Analyzer

For the impedance sensing system, a commercial IC chip with a part number of AD5933 from ADI serves as the core part for this system [16]. It is a widely used network analyzer IC for impedance measurement. The functional block diagram of the AD5933 is shown in Figure 3.3.

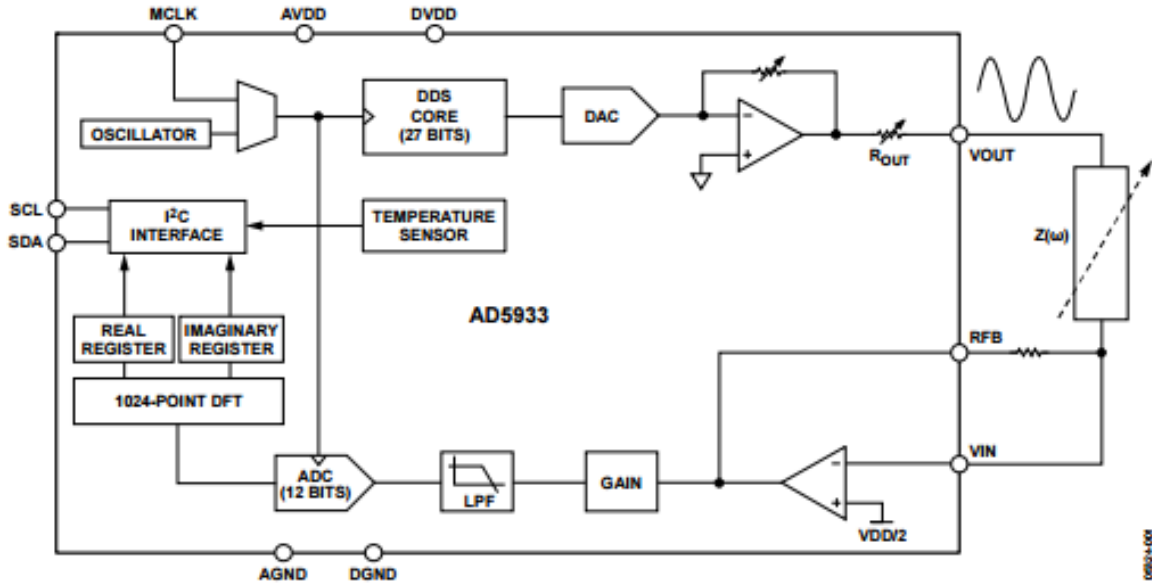


Figure 3.3: Functional block diagram of AD5933 [16]

This chip measures the impedance of the unknown target by applying a known frequency. An on-board DSP engine processes the response signal from the target impedance by sampling it through the on-board ADC and DFT [16]. The real and imaginary data for the impedance at each frequency point along the sweep can be extracted to calculate the impedance magnitude and phase by applying the equations 1.3 and 1.4.

The frequency sweep can be programmed by the users to define start frequency, frequency resolution, and number of points in the sweep through serial I2C interface. The DDS is used for

setting the start frequency and frequency increment by programming the corresponding register address. The formula for generating the required code loaded to the registers is shown in equation 3.1, where MCLK is the master clock frequency, the oscillator frequency.

$$\text{Start Frequency Code} = \left( \frac{\text{Required Output Start Frequency}}{\left( \frac{MCLK}{4} \right)} \right) \times 2^{27} \quad (3.1)$$

Also, the users can program the peak-to-peak amplitude of the output sine wave for the excitation to the unknown impedance. After the frequency sweep applies the unknown impedance, a current is developed and flows into the current-to-voltage converter. By a programmable gain amplifier, the voltage signal is amplified by a factor of 5 or 1 based on the users' settings. Then, the signal is low-pass filtered and converted to the digital data by passing the 12-bit ADC. Next, the DSP core of the AD5933 would perform a DFT on the sampled data by applying the equation 3.2, where:

$X(f)$  is the power in the signal at the frequency point  $f$ .

$X(n)$  is the ADC output.

$\cos(n)$  and  $\sin(n)$  are the sampled test vectors provided by the DDS core at frequency point  $f$ .

$$X(f) = \sum_{n=0}^{1023} (x(n)(\cos(n) - j \sin(n))) \quad (3.2)$$

After 1024 samples are accumulated for each frequency point, the impedance result is stored in two 16-bit registers as the real and imaginary parts. However, before measuring the unknown impedance, a known impedance component, a resistor in this system, should be calibrated for the gain factor calculation. Once the gain factor has been calculated, it could be used for unknown impedance calculation. The gain factor can be calculated by the equation 3.3, where

the impedance is known, and the magnitude can be calculated by the equation 1.3. Then, the unknown impedance can be calculated by applying the equation 3.4.

$$Gain\ Factor = \frac{(\frac{1}{Impedance})}{Magnitude} \quad (3.3)$$

$$Impedance\ to\ be\ measured = \frac{1}{Gain\ Factor \times Magnitude} \quad (3.4)$$

For the phase of the unknown impedance, the method is very similar to that for measuring the magnitude. First of all, a calibration resistor is needed for the system phase measurement. Then, after inserting the unknown impedance, the new phase is measured, and the phase of the unknown impedance can be calculated by the equation 3.5, where:

$Z\emptyset$  is the impedance phase.

$\Phi_{unknown}$  is the phase of the system with the unknown impedance.

$\nabla_{system}$  is the phase of the system with the calibration resistor.

$$Z\emptyset = (\Phi_{unknown} - \nabla_{system}) \quad (3.5)$$

### 3.3 Other Units and Components in System

To perform the lower frequency sweep for the AD5933, a clock generator (ADF4001) from ADI is used with a reference crystal oscillator. By setting the reference counter in Arduino through the GPIOs, the clock frequency is programmable. Although the AD5933 has an internal crystal oscillator, which has 16.776 MHz frequency [16], the impedance results for the lower frequencies generated by the internal crystal oscillator are less accurate than using a lower

frequency crystal. Thus, the system can be programmed to measure the impedance under the lower frequencies generated by the external crystal oscillator and to use its internal crystal oscillator to measure the impedance for higher frequencies.

To minimize the noise for the clock generated by the ADF4001 and external crystal oscillator, a D flip-flop is used. Also, the D flip-flop can help degrade the external master clock frequency. In the system, a 10 MHz crystal oscillator is applied. After the R-Counter in the ADF4001 and D flip-flop, the clock frequency is 2.5 MHz. Since the calibration resistor is embedded on the board, an analog multiplexer with a part number ADG884 from ADI is used.

When the unknown impedance is presented to the AD5933, a capacitor is put in series with the frequency signal because when the frequency varies, the DC offset for the signal also changes, which will cause inaccurate current flow through the unknown impedance. The capacitor can be used for filtering out the DC offset, and another constant DC offset 2.5 V is added to the signal.

For the power supply, all the VDD is supplied by the standard 5 V from the Arduino UNO board. The Arduino UNO board is powered either from a 3.7 V Li-ion battery with a Boost converter or the USB connector. Since the supply voltage range for the Arduino is 7-12 V, a Boost converter is needed to convert 3.7 V to at least 7 V with high efficiency. Also, USB battery charger for the Li-ion battery is implemented in the system. The schematic for the battery charger is shown in Figure 3.4. The circuit board has a micro USB header to connect the USB, and a slide switch for controlling the power supply of the whole system.



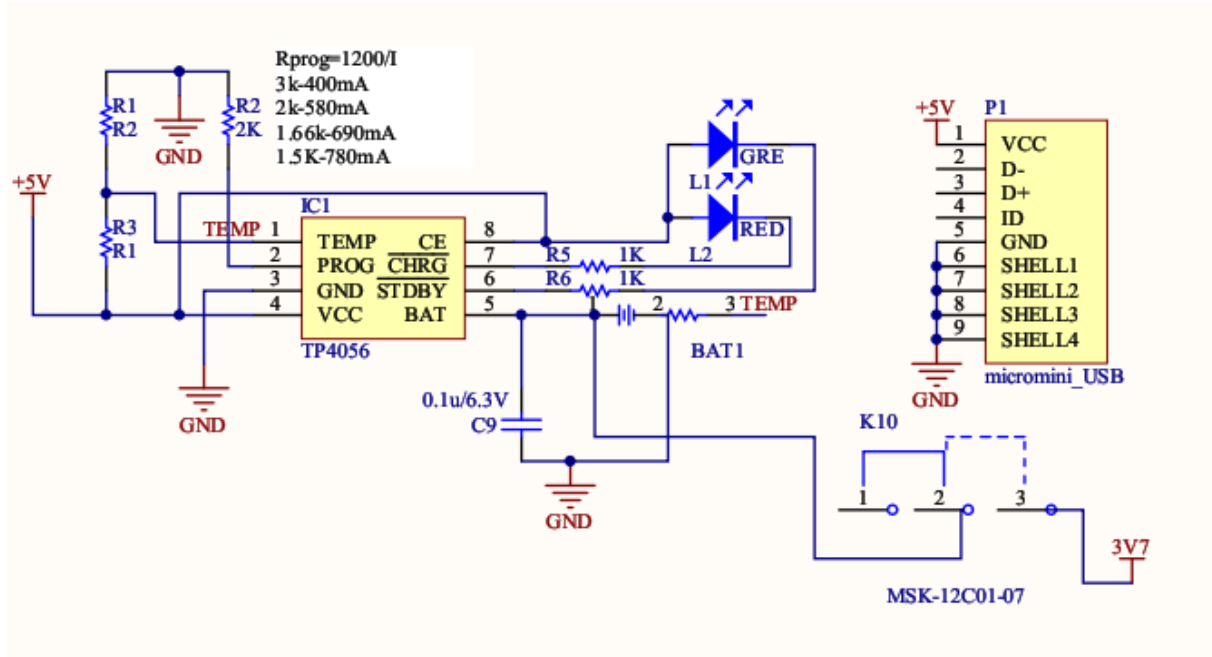


Figure 3.4: Li-ion battery charger schematic

### 3.4 Result

For E. coli, the impedance for this bacteria is in a range from 10 k $\Omega$  to 50 k $\Omega$ . Based on this information, RFB and R6 in the schematic from Figure 3.2 should be changed to 100 k $\Omega$  and 47 k $\Omega$  respectively for more accurate results. Also, the op-amp in the schematic should be changed to the same op-amp in the MoboSens system, which is the AD8667. After the changes are applied, by using a 100 k $\Omega$  calibration resistor and an external crystal oscillator, a 330 k $\Omega$  resistor and a 10 k $\Omega$  were tested under low frequency range, and the results are tabulated in Tables 3.1 and 3.2. Also, for the high frequency range powered by the internal oscillator, 330 k $\Omega$  and 10 k $\Omega$  resistors were tested by using a 100 k $\Omega$  calibration resistor, and the results are tabulated in Tables 3.3 and 3.4.

Table 3.1: 100 k $\Omega$  Calibration Resistor, 330 k $\Omega$  Test Resistor for 1 kHz to 15 kHz

| Frequency (kHz) | Cali_mag | Cali_phase (°) | Impedance ( $\Omega$ ) | Phase (°) |
|-----------------|----------|----------------|------------------------|-----------|
| 1               | 1388.54  | 4.77           | 301532.87              | 2.03      |
| 1.1             | 1337.73  | 4.76           | 319037.96              | -2.09     |
| 1.2             | 1332.91  | 4.78           | 320727.00              | 2.31      |
| 1.3             | 1361.46  | 4.78           | 309438.87              | -0.95     |
| 1.4             | 1357.54  | 4.78           | 325217.90              | -2.49     |
| 1.5             | 1349.53  | 4.80           | 328121.28              | 0.55      |
| 1.6             | 1360.45  | 4.79           | 319909.06              | 0.91      |
| 1.7             | 1332.16  | 4.81           | 326362.53              | 1.40      |
| 1.8             | 1331.46  | 4.81           | 324594.81              | -0.03     |
| 1.9             | 1340.02  | 4.81           | 326439.06              | 0.16      |
| 2               | 1338.13  | 4.81           | 322374.53              | -0.51     |
| 3               | 1338.89  | 4.87           | 330201.96              | 0.14      |
| 4               | 1323.32  | 4.92           | 315686.31              | 2.75      |
| 5               | 1333.91  | 4.99           | 325441.03              | 0.03      |
| 6               | 1344.35  | 5.04           | 339066.25              | -1.04     |
| 7               | 1330.51  | 5.09           | 329786.28              | 0.52      |
| 8               | 1338.75  | 5.14           | 325870.09              | -0.67     |
| 9               | 1339.13  | 5.20           | 323339.78              | 1.30      |
| 10              | 1349.04  | 5.26           | 336237.62              | -1.52     |
| 11              | 1336.35  | 5.31           | 321935.53              | 1.66      |
| 12              | 1338.32  | 5.37           | 322109.81              | 0.02      |
| 13              | 1339.19  | 5.38           | 360745.87              | 8.73      |
| 14              | 1330.25  | 5.48           | 322820.40              | 0.65      |
| 15              | 1299.74  | 5.51           | 348731.15              | 1.89      |

Table 3.2: 100 k $\Omega$  Calibration Resistor, 10 k $\Omega$  Test Resistor for 1 kHz to 15 kHz

| Frequency (kHz) | Cali_mag | Cali_phase (°) | Impedance ( $\Omega$ ) | Phase (°) |
|-----------------|----------|----------------|------------------------|-----------|
| 1               | 1390.19  | 4.77           | 10262.05               | -0.24     |
| 1.1             | 1346.26  | 4.77           | 9980.85                | -0.12     |
| 1.2             | 1352.67  | 4.77           | 10020.14               | -0.04     |
| 1.3             | 1373.36  | 4.78           | 10170.20               | -0.17     |
| 1.4             | 1344.22  | 4.78           | 9953.71                | 0.18      |
| 1.5             | 1340.65  | 4.80           | 9930.14                | -0.72     |
| 1.6             | 1355.63  | 4.79           | 10038.99               | 0.11      |
| 1.7             | 1338.14  | 4.81           | 9924.06                | -0.39     |
| 1.8             | 1347.88  | 4.81           | 9988.80                | -0.31     |
| 1.9             | 1349.18  | 4.81           | 9992.32                | -0.21     |
| 2               | 1335.94  | 4.81           | 9895.14                | 0.19      |
| 3               | 1336.41  | 4.87           | 9909.23                | -0.08     |
| 4               | 1337.63  | 4.92           | 9921.36                | 0.18      |
| 5               | 1342.61  | 4.98           | 9949.25                | -0.11     |
| 6               | 1324.37  | 5.03           | 9833.17                | -0.25     |
| 7               | 1338.69  | 5.09           | 9934.25                | -0.07     |
| 8               | 1367.16  | 5.13           | 10152.07               | 0.56      |
| 9               | 1342.12  | 5.20           | 9964.63                | -0.40     |
| 10              | 1328.45  | 5.24           | 9864.14                | 0.11      |
| 11              | 1328.92  | 5.31           | 9862.74                | -0.75     |
| 12              | 1333.49  | 5.37           | 9901.29                | -1.19     |
| 13              | 1360.92  | 5.39           | 10133.45               | 1.03      |
| 14              | 1325.52  | 5.47           | 9853.60                | -0.64     |
| 15              | 1310.53  | 5.51           | 9738.51                | -0.08     |

Table 3.3: 100 k $\Omega$  Calibration Resistor, 330 k $\Omega$  Test Resistor for 25 kHz to 100 kHz

| Frequency (kHz) | Cali_mag | Cali_phase (°) | Impedance ( $\Omega$ ) | Phase (°) |
|-----------------|----------|----------------|------------------------|-----------|
| 25              | 1947.83  | 1.81           | 320087.50              | -5.89     |
| 35              | 1937.85  | 1.91           | 312942.15              | -7.98     |
| 45              | 1955.42  | 2.01           | 310408.78              | -9.86     |
| 55              | 1963.74  | 2.09           | 311154.59              | -9.19     |
| 65              | 1947.31  | 2.20           | 302867.37              | -14.19    |
| 75              | 1930.93  | 2.30           | 302397.81              | -17.01    |
| 85              | 1944.98  | 2.40           | 293869.06              | -17.60    |
| 95              | 1914.55  | 2.48           | 276615.50              | -20.38    |
| 100             | 1962.72  | 2.57           | 273671.75              | -23.00    |

Table 3.4: 100 k $\Omega$  Calibration Resistor, 10 k $\Omega$  Test Resistor for 25 kHz to 100 kHz

| Frequency (kHz) | Cali_mag | Cali_phase (°) | Impedance ( $\Omega$ ) | Phase (°) |
|-----------------|----------|----------------|------------------------|-----------|
| 25              | 1955.34  | 1.81           | 11152.99               | 2.71      |
| 35              | 1948.40  | 1.91           | 11124.47               | 3.42      |
| 45              | 1951.60  | 2.01           | 11151.99               | 4.24      |
| 55              | 1964.70  | 2.11           | 11250.26               | 5.02      |
| 65              | 1952.74  | 2.20           | 11210.25               | 6.53      |
| 75              | 1956.72  | 2.29           | 11256.39               | 7.76      |
| 85              | 1952.11  | 2.40           | 11257.21               | 8.31      |
| 95              | 1965.95  | 2.48           | 11374.75               | 9.92      |
| 100             | 1900.00  | 2.57           | 11100.28               | 10.91     |

For the 330 k $\Omega$  test resistor under low frequency range, the average of the measured impedance is 326.072 k $\Omega$  with a 1.19% error, which is pretty close to the actual value. The error for the phase is also very small, which is 0.6563° with a 0.18% error. For the 10 k $\Omega$  test resistor under

low frequency range, the average of the measured impedance is  $9.966\text{ k}\Omega$  with a 0.344% error, which is pretty close to the actual value. The error for the phase is also very small, which is  $-0.142^\circ$  with a 0.04% error.

For the test resistors under high frequency range, it can be easily observed that both magnitude and phase have a larger error compared with the low frequency range. Thus, the lower frequency's data is more accurate than the higher frequency. Moreover, from the tables, the error for both magnitude and phase is smaller for the test resistor with a smaller value, especially for the high frequency range.

## **CHAPTER 4**

### **SUMMARY AND FUTURE WORK**

In summary, the MoboSens system and the impedance sensing system are demonstrated for portably rapid electrochemical and biomedical measurement. All the system-level circuit designs were tested on the breadboard. The components in the systems were verified to ensure that the system was fully functional and able to accurately characterize the electrochemical cells and biomedical bacteria.

For the next generation of MoboSens system, to increase its lifetime is always necessary. In the future, the buck converter can be replaced by a buck-boost converter or a boost converter, using a 3.7 Li-ion battery or AA batteries as their power source due to their larger capacity of charge. Since the semiconductor industry is always progressing, it is worth trying the latest IC chips with robust functionalities if available.

In the impedance sensing system, a battery gauge can be used for monitoring the battery state of charge since it is powered by a 3.7 Li-ion battery. The battery gauge can help to prevent deeply discharging and overcharging, so that increases the battery life. Also, an Arduino nano can be used to replace the UNO board due to its smaller form factor. Moreover, the cloud can be used for data storage and communication instead of the Bluetooth so that the impedance sensing information can be accessed by wi-fi, which has greater available distance.

## REFERENCES

- [1] Fajerwerg, K. (2010, October). An original nitrate sensor based on silver nanoparticles electrodeposited on a gold electrode. *Electrochemistry Communications*, 12(10), 1439-1441.
- [2] Sharpe, S. (n.d.). What is nitrite poisoning in aquarium fish? Retrieved from <http://freshaquarium.about.com/cs/disease/p/nitritepoison.htm>
- [3] Moorcroft, M. (2001). Detection and determination of nitrate and nitrite: A review. *Talanta*, 54(5), 785-803. doi:10.1016/s0039-9140(01)00323-x
- [4] Vashist, S. (2014, May). Cellphone-based devices for bioanalytical sciences. *Analytical and Bioanalytical Chemistry*, 406(14), 3263-3277.
- [5] Ozcan, A. (2014). Mobile phones democratize and cultivate next-generation imaging, diagnostics and measurement tools. *Lab on a Chip*, 14(17), 3187-3194.
- [6] Potentiostat Fundamentals. (n.d.). Retrieved from <http://www.gamry.com/application-notes/instrumentation/potentiostat-fundamentals/>
- [7] Electrical impedance. (n.d.). Retrieved from [https://en.wikipedia.org/wiki/Electrical\\_impedance](https://en.wikipedia.org/wiki/Electrical_impedance)
- [8] Herman P. Schwan. (n.d.). Retrieved from [https://en.wikipedia.org/wiki/Herman\\_P.\\_Schwan](https://en.wikipedia.org/wiki/Herman_P._Schwan)

- [9] Schwan, H. P. (1955). Electrical Properties of Body Tissues and Impedance Plethysmography. *IRE Transactions on Medical Electronics, PGME-3*, 32-46.  
doi:10.1109/iret-me.1955.5008535
- [10] Basic Analog Circuits. (2015, April 21). Retrieved from <http://www.ni.com/white-paper/3037/en/>
- [11] Laboratory of spectroscopy of defect structures ISSP RAS. (n.d.). Retrieved from <http://www.issp.ac.ru/llds/en/methods/impedance.html>
- [12] CD4046B (ACTIVE). (n.d.). Retrieved from <http://www.ti.com/product/CD4046B>
- [13] Analog Devices. (n.d.). Retrieved from <http://www.analog.com/en/products/amplifiers/operational-amplifiers/low-input-bias-current-amplifiers/ad8669.html>
- [14] SN74109 (OBSOLETE). (n.d.). Retrieved from <http://www.ti.com/product/SN74109>
- [15] Zhang, D., Lu, Y., Zhang, Q., Liu, L., Li, S., Yao, Y., Jiang, J., Liu, G., Liu, Q. (2016). Protein detecting with smartphone-controlled electrochemical impedance spectroscopy for point-of-care applications. *Sensors and Actuators B: Chemical*, 222, 994-1002.  
doi:10.1016/j.snb.2015.09.041
- [16] Analog Devices. (n.d.). Retrieved from <http://www.analog.com/en/products/rf-microwave/direct-digital-synthesis/ad5933.html>